JMATPRO	Journal of Advanced Materials and Processing 10 (1): 3-12, Winter 2022 http://jmatpro.iaun.ac.ir 20.1001.1.2322388.2022.10.1.1.4

Research Paper

Electromagnetic Waves Absorption of the Epoxy Resin-MWCNT Composite Synthesis via Ultrasonic Bath and Milling Process

Sadegh Shahriyari[1], Mahdi Omidi[1*], Seyyed Ali Hassanzadeh-Tabrizi[1], Mahdi Yeganeh[2], Hamid Reza Bakhsheshi-Rad[1]

1. Advanced Materials Research Center, Department of Materials Engineering, Najafabad Branch, Islamic Azad University, Najafabad, Iran

2. Department of Materials Science and Engineering, Faculty of Engineering, Shahid Chamran University of Ahvaz, Ahvaz, Iran

ARTICLE INFO

Article history:

Received 19 October 2021
Accepted 23 December 2021
Available online 1 January 2022

Keywords:
Electromagnetic waves absorption
MWCNT
Epoxy resin
Ultrasonic
Composite

ABSTRACT

In this study, ultrasonic bath and milling processes were used to synthesis epoxy resin-multiwalled carbon nanotubes (MWCNT) composite, and their effect on the absorption of magnetic waves was investigated using the Vector Network Analyzer (VNA) test. The effect of the concentration of MWCNT used to attract the wave's magnetic part in the epoxy resin matrix is also investigated. This study showed that the optimal amount of MWCNT in this epoxy resin-MWCNT composite was about 5 wt.% for the ultrasonic bath method, while it was around 15 wt% for the milling method. The ultrasonic bath caused the reflection losses (RL) value reaches to about -25 dB in the range of 9 to 11 GHz. The results of the VSM test showed that the composite produced from epoxy resin and MWCNT is a soft magnetic material. Also, the sample produced in the ultrasonic bath process has a higher magnetic saturation than the milling process, which causes it to absorb more electromagnetic waves.

Citation: Shahriyari, S.; Omidi, M; Hassanzadeh-Tabrizi, S.A.; Yeganeh, M.; Bakhsheshi-Rad, H.R. (2022) Electromagnetic Waves Absorption of the Epoxy Resin-MWCNT Composite Synthesis via Ultrasonic Bath and Milling Process, Journal of Advanced Materials and Processing, 10 (1), 3-12. Dor: 20.1001.1.2322388.2022.10.1.1.4

[*] **Corresponding Author**
E-mail Address: m_omidi@iaun.ac.ir

1. Introduction

Today's world relies heavily on technologies based on electromagnetic radiation, which is one of the most fundamental phenomena of nature. With the advancement of technology, unexpected problems are created for human health. For example, the more devices containing electromagnetic waves are used, the more human health is threatened. Since electromagnetic waves have many applications in the GHz frequency range for mobile phones, communication networks, radar systems, etc., protection against waves in this range is essential for humans [1-6]. Electromagnetic absorbers are among the most fundamental parts of wireless communications, etc., which have attracted much attention in the last decade [7-9]. These materials reduce the amount of reflected wave energy, thereby attenuating electromagnetic waves. Electromagnetic absorbers are used as microwave absorbers and for shielding applications. Absorbents must have properties that enhance their performance, including a) high absorption of electromagnetic waves in the high-frequency range, b) the electromagnetic wave absorbent material must be thin thickness, c) the absorption range of the absorbent material should cover the wide frequency range, d) other properties of the adsorbent materials include their high mechanical strength and low weight, e) it must also have high thermal and chemical stability and f) Finally, low production costs can be mentioned as a feature for electromagnetic wave absorbers [10-14].

An electromagnetic wave absorber is a substance that attenuates the electromagnetic energy emitted, and there are generally two views on the absorption of electromagnetic waves. Microscopically, the performance of materials in electromagnetic fields is determined by the displacement of free electrons and their bonding in the electric field and the direction of their atomic motions in the magnetic field. According to Maxwell's equations, the adsorption rate of the adsorbent can be measured [10, 11]. From a macroscopic point of view, the reaction of materials (absorption and reflection) against electromagnetic waves is determined by three related parameters, electrical conductivity ($\varepsilon^* = \varepsilon' - i\varepsilon''$), magnetic permeability ($\mu^* = \mu' - i\mu''$), and electrical conductivity (σ) [12]. The (μ' , ε') real parts are related to storage, and (μ'', ε'') the imaginary parts are related to the dissipation of electromagnetic waves. Also, the imaginary part ratio to the real part is equal to the material loss factor [13]. The wave absorber must have wave resistance to dissipate it [14]. The wave resistance is defined by impedance and is presented in the following Equation (1):

$$z_{in} = \frac{z_{in}}{z_0} = \sqrt{\frac{\mu}{\varepsilon \tanh\left[-i2\pi\frac{d}{\lambda}\sqrt{\varepsilon\mu}\right]}} \quad (1)$$

where, μ, ε are magnetic permeability and dielectric permeability, respectively. It was worth noting that d, thickness, and λ are also the wavelengths of free space. By calculating the input impedance, the reflective loss is also obtained, which is presented in Equation (2):

$$RL(dB) = -20\,log\left(\frac{z_{in}-1}{z_{in}+1}\right) \quad (2)$$

Wave absorbers are typically selected from intermediate metals, oxides, hydroxides, nanoparticles, nanotubes, conductive polymers, and composites. These nanocomposites include conductive polymers (absorbers of the electric wavelength) and magnetic particles (absorbers of the magnetic wavelength) dispersed in the polymer matrix. When the dimensions of the structures of mineral compounds are reduced to the nanoscale, they have significant effects on their mechanical, optical, electrochemical, and thermal properties and the absorption of their electromagnetic waves [15-22]. Currently, epoxy resin-MWCNT composites are employed as microwave absorbers for shielding applications. Applications of some of the structures and materials used in the field of electromagnetism are: electromagnetic wave absorbers, electrical shields, antenna designs, protection of humans and biomaterials against electromagnetic waves, and improved electromagnetic compatibility [16-22]. In one study, the effect of commercial multi-walled CNTs with different diameters and length-to-diameter ratios on X-band microwave adsorption, MWCNT epoxy nano-composite, prepared by ultrasonic methods and the ball mill was investigated. The research showed that the MWCNT with the largest aspect ratio resulted in composites with the highest X-band microwave absorption performance, which is considerably better than that of reported pristine CNT/polymer composites with similar or lower thicknesses and CNT loadings below 4 wt% [23]. In this paper, we tried to investigate the effect of carbon nanotubes in a polymer matrix and the existence of different intermediate processes, including ultrasonic baths and the milling process, which affects the separation of nanotubes. Finally, this study aims to fabricate a nanocomposite from epoxy-MWCNT resin and to investigate the absorption power of electromagnetic waves at the scale of 12-8 GHz.

2. Materials and methods

In the present study, multi-walled carbon nanotubes with dimensions of 25 nm in diameter and 10 μm in length were used. The nanotubes used in this study were produced by the United Nanotech Innovations company (UNI), with purity and theoretical density of around 98% and 0.14 g/cm^3, respectively. Figure 1 shows the histogram and morphology of the nanotubes. It can be seen that the nanotubes are intertwined strands with dimensions of approximately 40 nm.

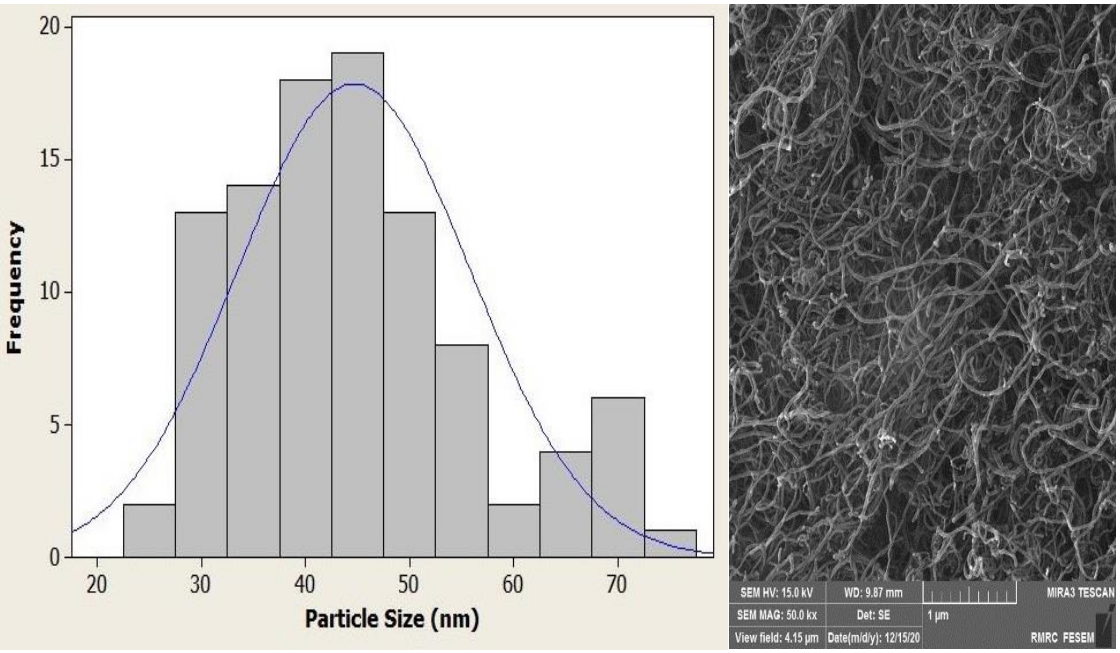

Fig. 1. Histogram and SEM image of MWCNTs powders.

The epoxy resin selected in this study consists of two components, EPL 1012 based on Bisphenol F-type and EPH112 as a hardener, listed in Table 1. Its low viscosity allows for complete impregnation of reinforcement fibers like glass, carbon, and aramid or mineral powder such as silica and makes it suitable for processing methods such as wet lay-up and Resin transfer molding (RTM).

Table 1. The thermal and physical properties of epoxy resin.

Properties	Amount	Unit	Standard
Volume Electrical Strength	$1.8*10^{15}$	Ohm.cm	ASTM D257
Surface Electrical Strength	$9.5*10^{12}$	Ohm	ASTM D257
Dielectric Constant	6	-	ASTM D150
Coefficient of Thermal Expansion	$6.2*10^{-5}$	$(C^0)^{-1}$	ASTM D864

In the present study, an ultrasonic bath and milling process was used to increase the absorption of electromagnetic waves. The carbon nanotubes were placed in a laboratory calibrated cylinder with 50 cc of ethanol. The carbon nanotubes and ethanol mixture was placed in an ultrasonic bath, and ultrasonic waves separated the nanotubes for 80 min. The frequency used in this step was set to 100 Hz. It is also worth noting that the milling process leads to an increase in the absorption of electromagnetic waves. A mixture of carbon nanotubes and ethanol was added to a steel cup. Stainless steel balls of four different sizes of 5, 7, 9, and 13 mm were used in the mixing process. The mixing process was performed wet, and the time used was one hour at 250 rpm in a planetary ball mill. To produce an epoxy resin-MWCNT composite, the weight values of the composite were calculated based on Equation 3:

$$m_C(gr) = (x)A + (1-x)B \quad (3)$$

where m_C is the weight of the composite in grams, A and B are the weight of the carbon nanotube and the composite matrix, respectively, X is the weight percentage of the reinforcing phase in the final composite. Also, in this formula, part B consists of two components, resin, and hardener, the ratio of which is shown in Equation 4.

$$B = \big((85\%)R + (15\%)H\big) \quad (4)$$

The resin is denoted by R and the hardener by H, and then, after mixing the composite materials in appropriate proportions in a sterile laboratory container for 3 min and using an electric mixer, they were mixed at a speed of 1000 rpm. After mixing, the resulting composite was placed in a drying oven. At this stage, to remove ethanol from the composite composition, a temperature of 110 °C and 24 hours were selected. At the end of the drying step, the sample was cut according to Waveguide (WR90) to perform the electromagnetic wave absorber test. The sample size for use in the networking analyzer (VNA) is 22.6 × 1.10 mm, and its thickness is equal to 5 mm. An electromagnetic wave absorption test was performed in the range of 8 to 12 GHz. A scanning electron microscope (SEM; MIRA3TESCAN-XMU) made by the TESCAN company in the Czech Republic

examined carbon nanotube morphology. Also, the VSM model LBKFB model of Meghnatis Daghigh Kavir Company in Iran investigated the material's magnetic state. In order to calculate the amount of electromagnetic waves absorption, a model networking analyst (VNA, HP 8410C) located in the antenna laboratory of Khajeh Nasir al-Din Tusi University has been selected. IR testing was performed by Bomem MB-Series FT-IR Spectrometer in MID-IR range.

3. Results and Discussion

Figure 2 exhibited the FTIR spectrum epoxy resin specimen without MWCNTs after drying and calcination. Regarding the epoxy resin, the absorption band indicative of the OH bond is observed between 3590 and 3180 cm^{-1}. Owing to the limited number of OH groups in this resin's molecule, the peak noticed is small. The epoxy group is indicated by the 908 cm^{-1} band (in the 947 to 865 cm^{-1} range), while the peak indicates the existence of an aromatic group at 1100 cm^{-1}. The bands at 2951 cm^{-1} and 2872 cm^{-1} are caused by the C–H stretching vibration of the methyl group, whereas the band at 2930 cm^{-1} is caused by the C–H stretching vibration of the methylene group. The methyl C–H in-plane bending symmetrical vibrations s and asymmetrical vibrations as are found at 1379 cm^{-1} and 1451 cm^{-1}, respectively.

At 1597 cm^{-1}, 1586 cm^{-1}, and 1498 cm^{-1}, the distinctive C=C stretching of the benzene ring could be observed. Peaks at 1232 cm^{-1} and 1028 cm^{-1} correlate to C–O stretching, which indicates the modified epoxy resin's molecular backbone. Figure 2b shows the FTIR spectra of epoxy resin samples containing MWCNTs, which revealed two additional peaks at 1696 cm^{-1} related to carbonyl groups (C=O) and 1397 cm^{-1} that related to carboxyl groups (–COO). These two peaks suggested that MWCNTs were effectively encapsulated into the epoxy matrix [24].

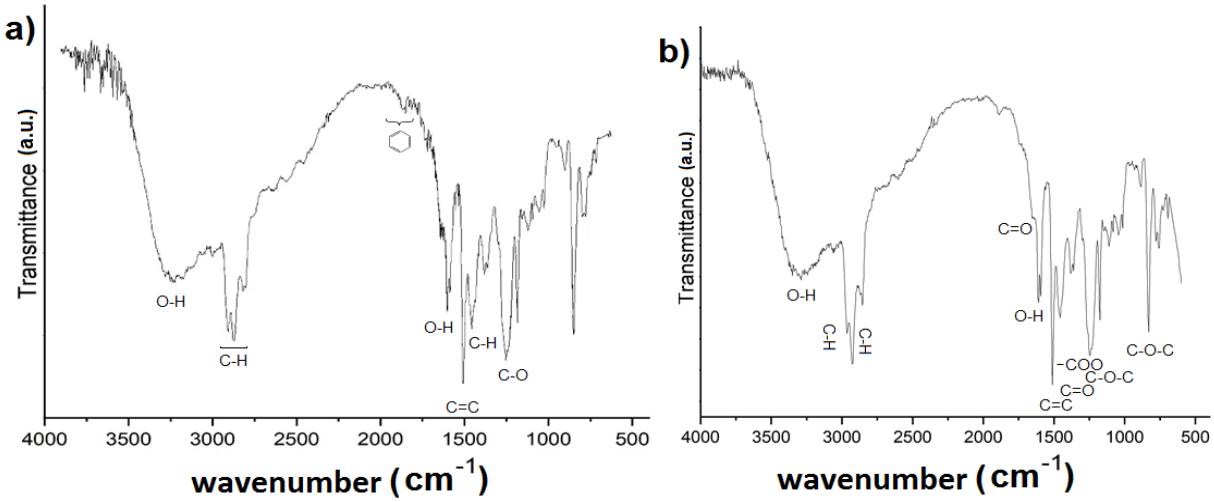

Fig. 2. The FTIR spectra of a) epoxy resin samples without MWCNTs and b) epoxy resin samples with MWCNTs

Figure 3 shows the results of the XRD test from ultrasonic and milling of the epoxy resin-MWCNT composite specimens. In both samples, the MWCNT peak is observed at an angle of 20 degrees. The MWCNT peak in the milling method has a decrease in intensity compared to the ultrasonic method. This decrease in intensity is due to the difference between the synthesis processes in these two samples. The result further confirms that there is no impurity in the synthesized specimens.

Figure 4 shows an electron microscope image of the sample surface with an ultrasonic bath's and no MWCNT agglomeration was seen on the sample surface. The samples prepared with the ultrasonic bath's intermediate stage have MWCNT with the same shape and original structure. Carbon nanotubes in this method of production do not have wall breakage middle stage. It was observed that the carbon nanotubes were well separated from each other, and crushing. Non-degradation of the nanotube structure will ensure that the electrical conductivity is maintained uniformly over a broader length and that the composite is more electrically homogeneous. Non-destruction and crushing of the wall of the multi-walled nanotubes in the sample with the intermediate stage of the ultrasonic bath reduced dislocation density. This reduction in dislocation density minimizes the electrical resistance of the sample [25, 26]. It should also be noted that with increasing MWCNT, the electrical conductivity increases as a result of reducing the level of insulated epoxy resin is reduced. This result has a good agreement with the result presented in the Ref. [21, 27-29].

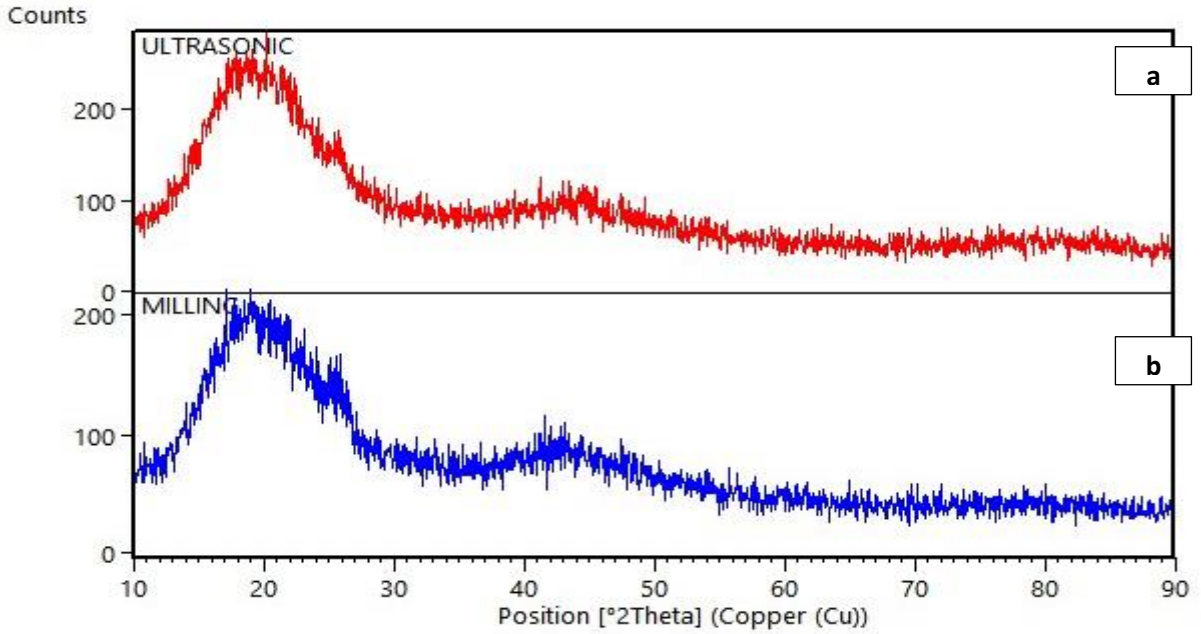

Fig. 3. XRD analysis of Epoxy resin-MWCNT composite: a) Ultrasonic method and b) Milling method

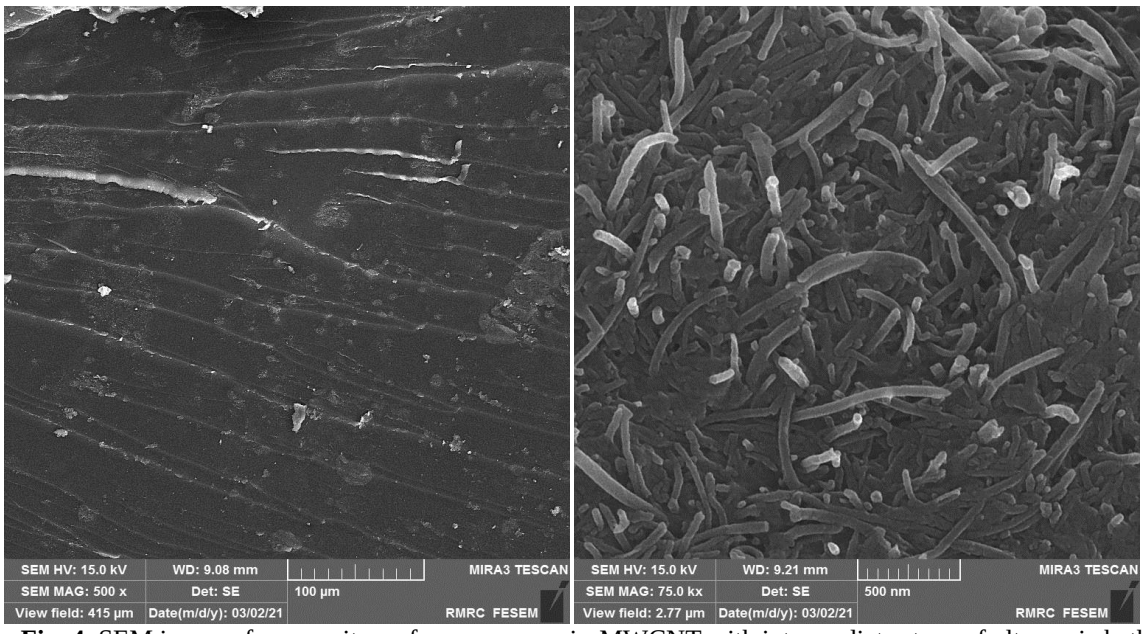

Fig. 4. SEM image of composite surface, epoxy resin-MWCNT with intermediate stage of ultrasonic bath

Figure 5 shows a scanning electron microscope image of the sample surface during the middle stage of the milling process. As seen in the image, the multi-walled carbon nanotubes are agglomerated and observed as an accumulation of nanotubes in the resin matrix. This occurred due to improper separation of the nanotubes by the middle stage of the mill process. Due to the successive blows of the steel bullets in the milling process, the image shows that the multi-walled carbon nanotubes suffered severe damage in structure and shape [30]. These damages can cause the composite's surface to not be fully integrated and homogeneous in electrical conductivity. Agglomeration can also severely affect the composite's electrical conductivity and eliminate electrical conductivity along the sample's entire length [30, 31].

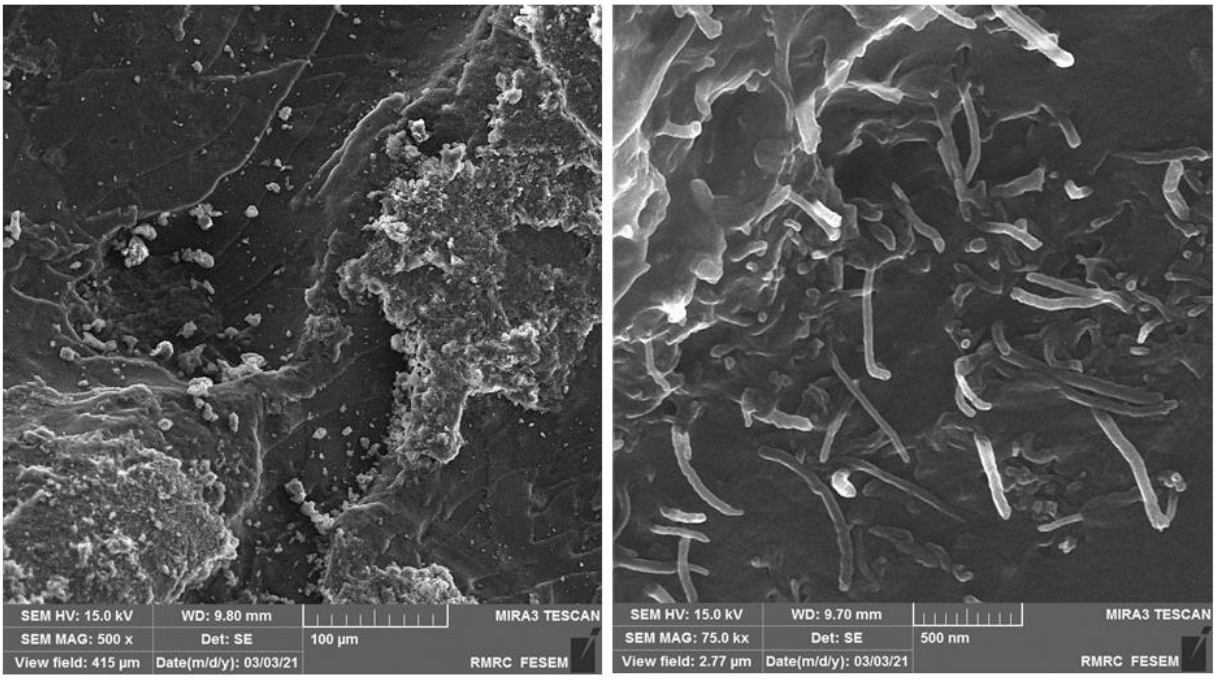

Fig. 5. SEM image of composite surface, epoxy resin-MWCNT with intermediate stage of milling process.

Figure 6 shows the results of the VSM test. In samples 6 (A) and 6 (B), epoxy resin and MWCNT composites with different intermediate stages underwent VSM testing, and it was observed that the results diagram was wholly changed and showed a soft magnetic material. Soft magnetic composite has properties well suited for absorbing magnetic waves, including meager coercive force, high permeability, high saturation of the core, and low residual magnetism. However, there is a slight difference between the two graphs. Figure 6 (A), which is related to the ultrasonic intermediate method, has a higher saturation magnet than 6 (B), which shows the hysteresis ring of the composite sample by the milling method. The reason for this saturation magnet is attributed to the uniform distribution of the MWCNT and lack of MWCNT agglomeration in the epoxy matrix after the milling process.

Figure 6 (C) shows that when the epoxy resin is placed in the magnetic field, its magnetic saturation is reduced, which reduces the absorption power of the magnetic part of the wave. It should be noted that magnetic and electric waves never exist alone, and the presence of each causes the emergence of the other. Since, in the VSM test, the field strength gradually increases and the epoxy resin is the only adsorbent of the electrical part of the wave, it is observed that the absorption of the magnetic part is significantly reduced. Then, when the presence of the field reaches zero, some magnetic residue is observed in the sample. The result revealed that the highest magnetic saturation at ($2500_{(Oe)}$) is related to the ultrasonic sample equal to ($0.1_{(emu/g)}$) and then for the milling sample ($0.075_{(emu/g)}$), and the lowest number is related to the epoxy resin sample with ($-0.01_{(emu/g)}$). As shown in the SEM images, the MWCNT distribution in the matrix of epoxy resin by the ultrasonic method is more uniform than in the milling method. This more uniform distribution and lack of MWCNT agglomeration in the epoxy matrix is the main reason for the higher saturation of the ultrasonic synthesized resin epoxy-MWCNT composite.

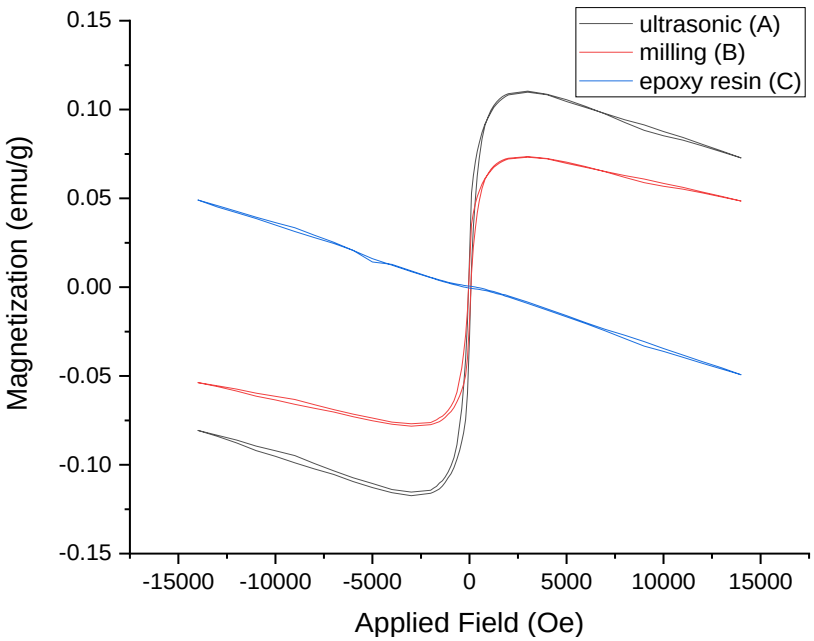

Fig. 6. VSM test results of composites produced, A) composites produced with ultrasonic bath's middle stage, B) composites produced with middle stage of milling process, C) Sample produced with epoxy resin without carbon nanotubes.

In order to investigate the absorption of electromagnetic waves, the reflection losses (RL) of the composites containing different amounts of carbon nanotube (0, 5, 10, 15, and 20 wt%) are shown in Figure 7. In this figure, the studied samples used ultrasonic waves to separate the carbon nanotubes. It was observed that the sample with 5 wt% of carbon nanotube has the highest reflection losses value. Also, this high RL value observed in the wide range between 9 to 11 GHz which is about -25 dB. It seems that increasing the concentration of carbon nanotubes by more than 5% by weight causes the nanotubes to not separate properly from each other. This unbalanced distribution of carbon nanotubes causes electrical conductivity not to be adequately maintained along the composite's entire length, which reduces the absorption of electromagnetic waves [32-34]. The 5 wt% sample mutation should be related to reaching the electrical conductivity threshold of epoxy resin–MWCNT nanocomposite [35]. Due to the proper distribution of carbon nanotubes in the resin matrix due to the separation of carbon nanotubes from each other by ultrasonic waves in the ultrasonic bath, the effective surface for magnetic wave absorption will increase. Proper distribution of nanotubes causes sequential reflections of electromagnetic waves in the resin epoxy-MWCNT nanocomposite [36].

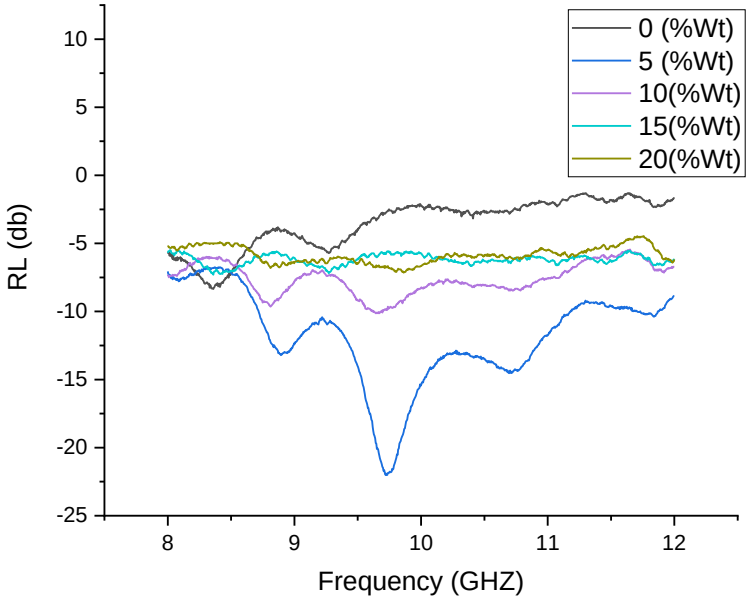

Fig. 7. The reflection losses of the composites containing different amounts of carbon nanotube produced with ultrasonic bath's middle stage: 0, 5, 10, 15, and 20 wt%

Carbon nanotubes will increase the electrical permeability of epoxy resin due to its very high electrical conductivity, which can help absorb electromagnetic waves [37-47]. Figure 8 shows the reflection losses (RL) of the composites containing different amounts of carbon nanotube produced with the middle stage of the milling process. As in Figure 8, all the produced composites showed a similar adsorption procedure in this diagram. However, the value of reflection losses of the produced composites by milling process is much lower than that of the samples with the intermediate ultrasonic bath process. Unlike the intermediate ultrasonic method, which had the highest adsorption at 5 wt%, the milling method had the highest RL value at 15 and 20 wt%. The impact of milling metal balls with carbon nanotubes in the milling method caused the carbon nanotubes to break. These collisions will shorten the length of the carbon nanotubes and break their walls. Reducing the nanotube walls' length and crushing will cause the nanotube network's integrity to be lost and cause the electrical conductivity not to form correctly.

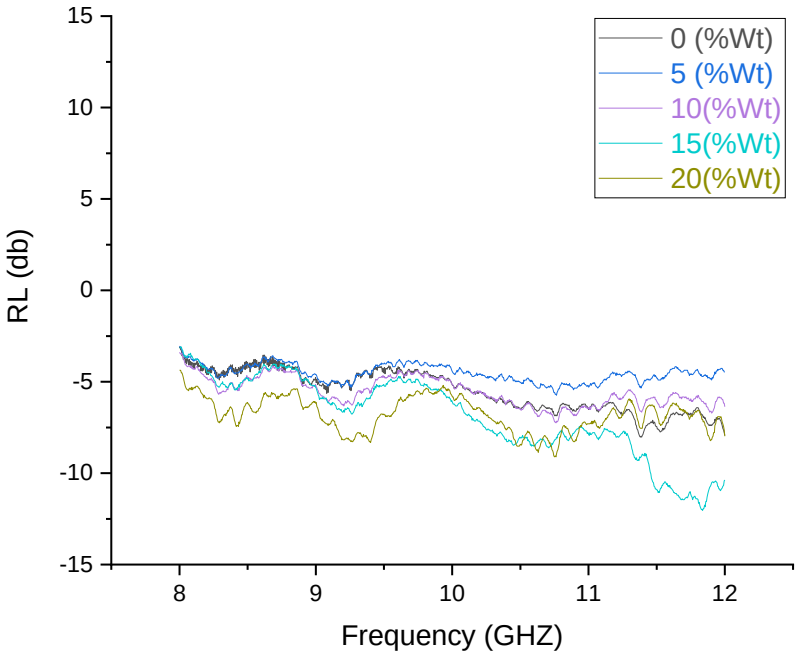

Fig. 8. The reflection losses of the composites containing different amounts of carbon nanotube produced with the middle milling stage: 0, 5, 10, 15, and 20 wt.%

4. Conclusions

According to the results obtained from the discussion and conclusion, it can be reported that:

1- The presence of compounds with two bands can help absorb the electrical part of the wave to absorb electromagnetic waves. In addition, the ultrasonic bath makes the MWCNT segregated more conveniently compared to the milling process.

2- Due to the absence of steel balls used in the milling process, the MWCNTs are not damaged in the ultrasonic intermediate process. Moreover, the production sample with the intermediate milling process causes areas with carbon nanotube agglomeration to be created.

3- The presence of carbon nanotubes that experienced mechanical damage and agglomeration reduces the electrical conductivity in the samples, which ultimately reduces the absorption of electromagnetic waves.

4- The highest reflection losses (RL) observed in the sample contains 5 wt.% carbon nanotubes, which were produced via the ultrasonic bath. Also, its maximum RL value range is 11-9 GHz and about -25 dB. Furthermore, the sample produced in the ultrasonic bath process has a higher magnetic saturation than in the milling process, which causes it to absorb more electromagnetic waves.

References

[1] J. Rushchitsky, Theory of waves in materials, ed., Bookboon, 2011.

[2] J. Cao, W. Fu, H. Yang, Q. Yu, Y. Zhang, S. Liu, P. Sun, X. Zhou, Y. Leng, S. Wang, B. Liu, G. Zou, "Large-scale synthesis and microwave absorption enhancement of actinomorphic tubular ZnO/CoFe2O4 nanocomposites". The Journal of Physical Chemistry B., Vol. 113, No. 14, 2009, pp. 4642-7.

[3] I.V. Shadrivov, M. Lapine, Y.S. Kivshar, Nonlinear, tunable and active metamaterials. Cham, Switzerland: Springer International Publishing; 2015.

[4] L. Peng, L. Li, R. Wang, Y. Hu, X. Tu, X. Zhong, " Microwave sintered Sr1− xLaxFe12− xCoxO19 (x= 0–0.5) ferrites for use in low temperature co-fired ceramics technology. Journal of Alloys and Compounds, Vol. 656, No. 2016, pp. 290-294.
[5] S. Lu, K. Ma, X. Wang, X. Xiong, W. Xu, C. Jia, " Fabrication and characterization of polymer composites surface coated Fe3O4/MWCNTs hybrid buckypaper as a novel microwave-absorbing structure. Journal of Applied Polymer Science, Vol. 132, No. 20, 2015, pp. 41974.
[6] I. Al Kawni, R. Garcia, S. Youssef, M. Abboud, J. Podlecki, R. Habchi, "Stabilization and encapsulation of magnetite nanoparticles", Materials Research Express, Vol. 3, No. 12, 2016, pp. 125024.
[7] N. Shiri, A. Amirabadizadeh, A. Ghasemi, "Influence of carbon nanotubes on structural, magnetic and electromagnetic characteristics of mnmgtizr substituted barium hexaferrite nanoparticles", Journal of Alloys Compounds, Vol. 690, No. 2017, pp. 759-764.
[8] X. Jian, B. Wu, Y. Wei, S.X. Dou, X. Wang, W. He, N. Mahmood, " Facile synthesis of Fe3O4/GCs composites and their enhanced microwave absorption properties. ACS Applied Materials & Interfaces, Vol. 8, No. 9, 2016, pp. 6101-6109.
[9] Z. Yan, J. Cai, Y. Xu, D. Zhang, "Microwave absorption property of the diatomite coated by Fe-CoNiP films". Applied Surface Science, Vol. 346, No. 2015, pp. 77-83.
[10] C.H. Papas, Theory of electromagnetic wave propagation, ed., Courier Corporation, 2014.
[11] M.F. Iskander, Electromagnetic fields and waves, ed., Prentice Hall, 1992.
[12] L.-F. Chen, C. Ong, C. Neo, V. Varadan, V.K. Varadan, Microwave electronics: Measurement and materials characterization, ed., John Wiley & Sons, 2004.
[13] X.C. Tong, Advanced materials and design for electromagnetic interference shielding, ed., CRC press, 2016.
[14] D. Micheli, C. Apollo, R. Pastore, M. Marchetti, "X-band microwave characterization of carbon-based nanocomposite material, absorption capability comparison and ras design simulation", Composites Science and Technology, Vol. 70, No. 2, 2010, pp. 400-409.
[15] X. Qi, Y. Deng, W. Zhong, Y. Yang, C. Qin, C. Au, Y. Du, "Controllable and large-scale synthesis of carbon nanofibers, bamboo-like nanotubes, and chains of nanospheres over Fe/SnO2 and their microwave-absorption properties". The Journal of Physical Chemistry C., Vol. 114, No. 2, 2010, pp. 808-814.
[16] M.-J. Park, J. Choi, S.-S. Kim, "Wide bandwidth pyramidal absorbers of granular ferrite and carbonyl iron powders", IEEE Transactions on Magnetics, Vol. 36, No. 5, 2000, pp. 3272-3274.
[17] E.F. Kuester, C.L. Holloway, "A low-frequency model for wedge or pyramid absorber arrays-i: Theory", IEEE Transactions on Electromagnetic Compatibility, Vol. 36, No. 4, 1994, pp. 300-306.
[18] C.L. Holloway, E.F. Kuester, "A low-frequency model for wedge or pyramid absorber arrays-ii: Computed and measured results", IEEE Transactions on Electromagnetic Compatibility, Vol. 36, No. 4, 1994, pp. 307-313.
[19] D.-A. Li, H.-B. Wang, J.-M. Zhao, X. Yang, "Fabrication and electromagnetic characteristics of microwave absorbers containing ppy and carbonyl iron composite", Materials Chemistry and Physics, Vol. 130, No. 1-2, 2011, pp. 437-441.
[20] A. Mandal, C.K. Das, " Effect of BaTiO3 on the microwave absorbing properties of Co-doped Ni-Zn ferrite nanocomposites ", Journal of Applied Polymer Science, Vol. 131, No. 4, 2014.
[21] Y. Zhai, Y. Zhang, W. Ren, "Electromagnetic characteristic and microwave absorbing performance of different carbon-based hydrogenated acrylonitrile–butadiene rubber composites", Materials Chemistry and Physics. Vol. 133, No. 1, 2012, pp. 176-181.
[22] T. Ting, Y. Jau, R. Yu, "Microwave absorbing properties of polyaniline/multi-walled carbon nanotube composites with various polyaniline contents", Applied Surface Science, Vol. 258, No. 7, 2012, pp. 3184-3190.
[23] B.Q.N. Bien Dong Che, Le-Thu T Nguyen, Ha Tran Nguyen, Viet Quoc Nguyen, Thang Van Le & Nieu Huu Nguyen "The impact of different multi-walled carbon nanotubes on the X-band microwave absorption of their epoxy nanocomposites", Chemistry Central Journal Vol. 9, No. 2015, pp.1-13.
[24] Z. Wu, S. Li, , M. Liu, Z. Wang and X. Liu,. Liquid oxygen compatible epoxy resin: Modification and characterization. RSC Advances, 2015, *5*(15), pp.11325-11333.
[25] S. Rathee, S. Maheshwari, A.N. Siddiquee, M. Srivastava, "A review of recent progress in solid state fabrication of composites and functionally graded systems via friction stir processing", J Critical Reviews in Solid State Materials Sciences, Vol. 43, No. 4, 2018, pp. 334-366.
[26] H. Li, A. Misra, Z. Horita, C.C. Koch, N.A. Mara, P.O. Dickerson, Y. Zhu, "Strong and ductile nanostructured cu-carbon nanotube composite", J Applied Physics Letters, Vol. 95, No. 7, 2009, pp. 071907.
[27] S. Barrau, P. Demont, E. Perez, A. Peigney, C. Laurent, C.J.M. Lacabanne, "Effect of palmitic acid on the electrical conductivity of carbon nanotubes−epoxy resin composites", Macromolecules. Vol. 36, No. 26, 2003, pp. 9678-9680.

[28] J. Sandler, M. Shaffer, T. Prasse, W. Bauhofer, K. Schulte, A.J.P. Windle, "Development of a dispersion process for carbon nanotubes in an epoxy matrix and the resulting electrical properties", Polymer. Vol. 40, No. 21, 1999, pp. 5967-5971.
[29] Y.S. Song, J.R.J.C. Youn, "Influence of dispersion states of carbon nanotubes on physical properties of epoxy nanocomposites", Carbon. Vol. 43, No. 7, 2005, pp. 1378-1385.
[30] H. Zhuang, G. Zheng, A. Soh, "Interactions between transition metals and defective carbon nanotubes", J Computational Materials Science, Vol. 43, No. 4, 2008, pp. 823-828.
[31] H. Kaurav, S. Manchanda, K. Dua, D.N. Kapoor, "Nanocomposites in controlled & targeted drug delivery systems", Proc. Nano Hybrids and Composites, 2018, pp. 27-45.
[32] J. Hernández, M.C. García-Gutiérrez, A. Nogales, D.R. Rueda, M. Kwiatkowska, A. Szymczyk, Z. Roslaniec, A. Concheso, I. Guinea, T.A. Ezquerra, "Influence of preparation procedure on the conductivity and transparency of swcnt-polymer nanocomposites", J Composites Science Technology, Vol. 69, No. 11-12, 2009, pp. 1867-1872.
[33] J. Li, P.C. Ma, W.S. Chow, C.K. To, B.Z. Tang, J.K. Kim, "Correlations between percolation threshold, dispersion state, and aspect ratio of carbon nanotubes", J Advanced Functional Materials, Vol. 17, No. 16, 2007, pp. 3207-3215.
[34] J. Aguilar, J. Bautista-Quijano, F.J.E.P.L. Avilés, "Influence of carbon nanotube clustering on the electrical conductivity of polymer composite films", Express Polym Lett. Vol. 4, No. 5, 2010, pp. 292-299.
[35] A.P. Singh, P. Garg, F. Alam, K. Singh, R. Mathur, R. Tandon, A. Chandra, S. Dhawan, "Phenolic resin-based composite sheets filled with mixtures of reduced graphene oxide, γ-Fe2O3 and carbon fibers for excellent electromagnetic interference shielding in the x-band", Carbon, Vol. 50, No. 10, 2012, pp. 3868-3875.
[36] H.-B. Zhang, Q. Yan, W.-G. Zheng, Z. He, Z.-Z. Yu, "Tough graphene− polymer microcellular foams for electromagnetic interference shielding", ACS Applied Materials & Interfaces, Vol. 3, No. 3, 2011, pp. 918-924.
[37] G. De Bellis, A. Tamburrano, A. Dinescu, M.L. Santarelli, M.S. Sarto, "Electromagnetic properties of composites containing graphite nanoplatelets at radio frequency", Carbon, Vol. 49, No. 13, 2011, pp. 4291-4300.
[38] P. Bhattacharya, C.K. Das, S.S. Kalra, "Graphene and mwcnt: Potential candidate for microwave absorbing materials", Journal of Materials Science Research, Vol. 1, No. 2, 2012, pp. 126.
[39] S.u.D. Khan, M. Arora, M.A. Wahab, P. Saini, "Permittivity and electromagnetic interference shielding investigations of activated charcoal loaded acrylic coating compositions", Journal of Polymers, Vol. 2014, No. 2014, Article ID 193058.
[40] A. Gharieh, M.S. Seyed Dorraji, "A systematic study on the synergistic effects of mwcnts and core–shell particles on the physicomechanical properties of epoxy resin", Scientific Reports. Vol. 11, No. 1, 2021, pp. 1-11.
[41] G. Hu, W. Fu, Y. Ma, J. Zhou, H. Liang, X. Kang, X.J.M. Qi, "Rapid preparation of MWCNTS/epoxy resin nanocomposites by photoinduced frontal polymerization", Materials. Vol. 13, No. 24, 2020, pp. 5838.
[42] S. Roy, R.S. Petrova, S.J.N.r. Mitra, "Effect of carbon nanotube (CNT) functionalization in epoxy-CNT composites", Nanotechnology reviews, Vol. 7, No. 6, 2018, pp. 475-485.
[43] M. Yazdi, V.H. Asl, M. Pourmohammadi, H. Roghani-Mamaqani, "Mechanical properties, crystallinity, and self-nucleation of carbon nanotube-polyurethane nanocomposites", Polymer Testing. Vol. 79, No. 2019, pp. 106011.
[44] M. Haghgoo, R. Ansari, M.J.C.P.B.E. Hassanzadeh-Aghdam, "Prediction of electrical conductivity of carbon fiber-carbon nanotube-reinforced polymer hybrid composites", Composites Part B: Engineering. Vol. 167, No. 2019, pp. 728-735.
[45] M.A. Zhilyaeva, E.V. Shulga, S.D. Shandakov, I.V. Sergeichev, E.P. Gilshteyn, A.S. Anisimov, A.G. Nasibulin, "A novel straightforward wet pulling technique to fabricate carbon nanotube fibers", Carbon. Vol. 150, No. 2019, pp. 69-75.
[46] H. Jintoku, Y. Matsuzawa, M.J.C. Yoshida, "Dual use of anionic azobenzene derivative as dispersant and dopant for carbon nanotubes for enhanced thermal stability of transparent conductive films", Carbon. Vol. 152, No. 2019, pp. 247-254.
[47] J. Pan, L.J.M.C. Bian, Physics, "A physics investigation for influence of carbon nanotube agglomeration on thermal properties of composites", Materials Chemistry and Physics. Vol. 236, No. 2019, pp. 121777.